OPTOELECTRONICS AND ADVANCED MATERIALS – RAPID COMMUNICATIONS Vol. 3, No. 6, June 2009, p. 581 - 585

Shape memory effect and related characteristics of helical springs made from Cu–Al–Ni alloy by investment casting

S. STANCIU, L.-G. BUJOREANU*, N. CIMPOESU, I. IONIȚĂ, V. MOLDOVEANU
Faculty of Materials Science and Engineering, the "Gh. Asachi" Technical University from Iaşi, Bd. D. Mangeron 61A, 700050 Iaşi, Romania

By means of displacement-temperature variation curves, the occurrence of work developing shape memory effect (SME) was revealed in the case of helical springs made from a Cu-Al-Ni shape memory alloy, obtained by investment casting. The corresponding critical temperatures of martensitic transformation, determined on springs trained by SME cycling, were compared to the results obtained by differential scanning calorimetry (DSC) and by dilatometry, on fragments cut from median coil of SMA springs, both in as-cast and in trained alloy. The microstructure of as-cast SMA springs was analyzed by scanning electron microscopy (SEM) in order to reveal martensite formation.

(Received February 13, 2009; accepted June 15, 2009)

Keywords: Cu-Al-Ni based shape memory alloys, Displacement-temperature curves, Investment casting, Critical transformation temperatures, Shape memory effect

1. Introduction

The most important functions of conventional metallic helical springs are force-generation and mechanical-shock damping [1]. Shape Memory Alloy (SMA) springs, able to generate work, provide an opportunity to develop a wide variety of thermally-sensitive actuators. With proper design, a shape memory spring can be used as a thermo-mechanical actuator to lift loads, to proportionally control a thermal system, or to operate thermal switches [2]. With suitable thermo-mechanical training, a 0.01 m-long TiNiCu SMA spring was able to develop two-way shape memory effect (TWSME) during thermal cycling over a 0.185 m stroke [3]. On the other hand, a 0.01276 kg-weighing Cu-Zn-Al lamellar helical spring developed a 0.232 m stroke while lifting a 3 N-load [4]. All these features recommend SMA springs as active elements for actuators in engineering applications [5] or even at robots for planetary exploration [6].

The load–deformation behaviour of SMA springs is best described in terms of material stiffness. β-type SMAs exhibit a large change in elastic modulus over a relatively narrow temperature range, increasing from low to high temperature [7]. The change in modulus with temperature is the result of a reversible martensite-to-austenite solid state phase transition. In martensitic state the spring is soft, being permanently deformed and does not return into its original length, stable stress-reoriented martensite plate variants being formed. When heated, stress-reoriented martensite becomes unstable, reverts to austenite and the spring recovers its undeformed state. In the classical actuation-scheme example, a SMA spring works against a strained steel spring. If the parameters of the springs are accurately chosen, the steel spring will compress the SMA spring at low temperature and will be compressed at its turn at high temperature [8]. In the absence of the steel spring its role can be played by an applied load (weight). The load will deform the SMA spring in martensitic condition and will be displaced by the spring in austenitic state, providing the stress caused by the weight will not exceed alloy's recovery stress. Thus, work-generating shape memory effect (SME) will be performed.

An important characteristic of the heating cooling behaviour of shape memory springs is thermal hysteresis. The hysteresis transformation loop offers information about both the macroscopic and the microscopic nature of the transformation. On one hand, theoretical transformation temperatures can be graphically determined, by so-called "tangent method" [2]. On the other hand, the width and the slope of the loop are indicative for the levels of internal friction and stored elastic energy, respectively [9].

Since SMA-spring obtaining requires the use of wire as raw material, which is subjected to rather complex mechanical processing [10] the present paper aims to introduce an alternative technology for springs manufacturing directly by casting and to evaluate their macroscopic behaviour and microscopic structure related to reverse martensitic transformation..

2. Experimental details

2.1 Production of as-cast SMA springs

An original manufacturing-technology for obtaining shape memory alloy springs made from Cu-12.89 Al-4.26 Ni (mass. %) under patent special protection

flux [11] was established, with the following main steps:

a) Fusible-model execution, using round stearin wires with 1.2×10^{-3} m diameter, for active coils and 3×10^{-3} m -thick lamellas, for casting network, as shown in Fig. 1(a). The stearin wire is whirled on a steel cylindrical calibre, with a helicoidally semi-round canal having the spring pitch.

b) Forming to obtain the hollow mould using Silicon powder (forming material for dental technique). Powder fluidization is made by water-mixing in a ratio 1:1, in a special elastomer-made crucible during 60 seconds with continuous stirring. Forming-mixture hardening takes 2.7 ksec and after that it is possible to take away the forming-frame.

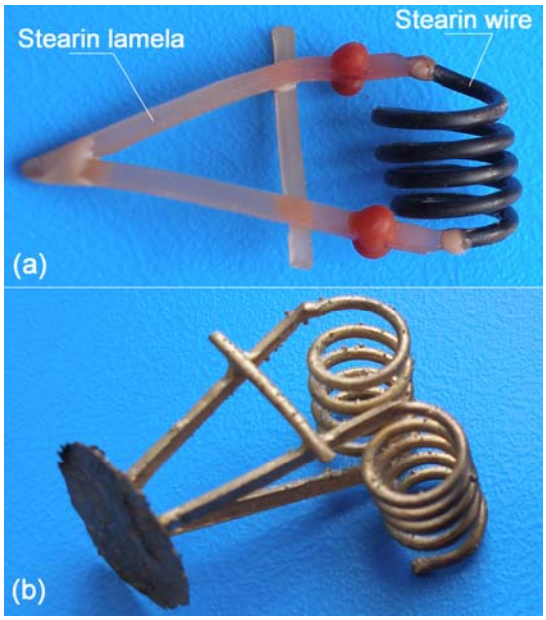

Fig. 1. Illustrations of different steps of the technology for SMA spring-obtainment: (a) fusible model; (b) as-cast spring assembly.

c) Heat treatment is applied in order to enable drying, hardening and final stabilization of form. First heat treatment-stage is performed in a special silit-rod furnace in order to achieve preliminary drying for 2×3.6 ksec at 470 K. After that, the form is quickly immersed in a hardening solution followed first by a very slow heating to 570 K (during almost one hour) and then by a normal heating to 1070 K with 2×3.6 ksec -maintaining in order to achieve dimensional stabilization before casting.

d) Casting involves fast alloy melting using a high frequency induction furnace (20 kHz). The alloy is first heated, in the silit-rod furnace to 1040 K and in this time the form is installed in the furnace inductor. After 30 seconds the alloy melts with intense homogenization under the effect of high-frequency induction currents. Immediately, the form is removed from induction furnace and installed in the support of a centrifugal-melting machine with mechanical actuation. This equipment was adapted after a model used for dental technique laboratories and has the advantage of reaching a maxim number of rotations in a very short time (least than a second) being designed for complex-piece casting with small dimensions in very short periods of time.

During centrifugation appreciable pressures are developed in the mould, as high as 200 MPa which force liquid alloy to infiltrate into the casting network and fill the form cavity from which melt stearin was expelled. To ensure a higher cooling rate, the equipment is turned off after a few seconds and the form is cooled in water. Finally, as-cast spring assemblies, as shown in Fig. 1(b), were obtained with 11×10^{-3} m-external diameter, 17×10^{-3} m-length and weighing 2×10^{-3} kg.

2.2 Characterization procedure

Displacement-temperature variation curves were recorded on a special device [12] under three applied loads (0.5 N, 1 N and 1.5 N, respectively) at an average heating rate of $4\times1.66\ 10^{-2}$ K/ sec developed by a special air-heater. Deformation was measured with an accuracy of $\pm0.1\cdot10^{-3}$ m. For temperature-measurement of the SMA springs, two multimeters were connected in parallel, one comprising a thermocouple and the other comprising a thermal diode [12]. During experiments the springs were subjected to SME cycling, comprising air-heating and air-cooling under load. It was estimated that training was completed after 20 SME cycles.

Calorimetric response of SMA springs was recorded by means of a NETZSCH STA 449 F3 device during a heating-cooling cycle between RT and 870 K, under Ar atmosphere, with a rate of $10\times1.66\ 10^{-2}$ K/s. Fragments were cut from the median coils of two SMA springs in as-cast and in trained condition, respectively.

Dilatometric measurements on lamellas cut from as-cast SMA springs, see Fig. 1(a), were performed on a NETZSCH DIL 402 CD dilatometer, during heating with $5\times1.66\ 10^{-2}$ K/s, under He atmosphere, up to 870 K. Fused silica and alumina were used as a sample holder material and a standard calibration material, respectively. For dilatometric evaluation the variations with temperature of $(dL/\ L_0)$ – relative thermal expansion; $d(dL/\ L_0)\ dt$ - relative thermal expansion derivative, representing expansion rate in time and (α) - thermal expansion coefficient were analyzed.

SEM micrographs were recorded by means of a SEM – VEGA II LSH TESCAN scanning electron microscope, coupled with an EDX – QUANTAX QX2 ROENTEC detector.

3. Experimental results and discussion

Closed displacement-temperature curves were obtained after applying 20 heating-cooling cycles, up to 705 K, performed under three different applied loads, as illustrated in Fig. 2. Close-loop obtainment is generally related to a fully reversible transformation, which means that SMA springs were trained after 20 SME cycles being able to perform extrinsic TWSME [13]. Critical temperatures for martensitic transformation were determined by the tangent

method, as shown in Fig. 2, for 1.5 N-load, the results being listed in Table 1.

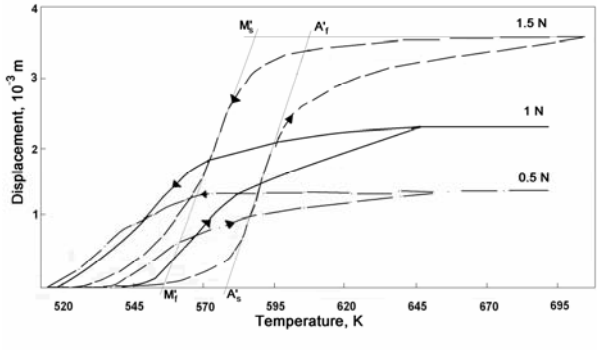

Fig. 2 Displacement-temperature closed diagrams of SMA springs, recorded at the end of training procedure, by SME-cycling up to 705 K, under the effect of three different applied loads.

As previously observed, at lamellar helical springs made of Cu-Zn-Al SMA, the variation rate of displacement with temperature as well as the stroke show an obvious increasing tendency with increasing the applied loads [4].

Table 1. Variation of critical temperatures (K) for martensitic transformation as a function of applied load, as determined from Fig. 2.

Load, N	M'_f	M'_s	A'_s	A'_f
0.5	519	556	539	589
1	528	579	550	604
1.5	556	590	580	609

When considering Clausius-Clapeyron equation, it is expected that critical temperatures increase, as well, with applied load [14]. Since maximum stroke reached 3.6×10^{-3} m, while lifting a load of 1.5 N, total developed work was 5.4×10^{-3} J which gives a specific output per mass unit of 2.7 J/ kg.

Fragments cut from median coils of SMA springs, both in as-cast and trained condition, were subjected to DSC analysis. Representative results are shown in Fig. 3.

In as-cast condition, Fig. 3(a) reveals three endothermic peaks (designated as *1-3*) and one exothermic peak (designated as *4*). According to our previous observations, it is assumed that peak *1* would correspond to low-temperature reverse martensitic transformation, peak *2* to high-temperature reverse martensitic transformation, peak *3* to eutectoid reaction and peak *4* to α-phase precipitation [15]. Since the fragment was cut from an undeformed spring, there should be no stress induced martensite and only thermally induced martensite is expected to occur after final water cooling, during the last step of manufacturing technology. Therefore peak *1* is rather bunt, possibly corresponding to the reversion to austenite of unstabilized thermally induced martensite while peak *2* is flat possibly due to retardation occurring in the reversion of stabilized thermally induced martensite to austenite. During subsequent heating, firstly eutectoid reaction and then α-phase precipitation are expected to occur corresponding to peaks *3* and *4*, respectively. Owing to α-phase precipitation, the matrix becomes depleted in copper, therefore richer in aluminium which causes marked decrease of critical temperatures for forward martensitic transformation [16]. For this reason no solid state transition is noticeable during subsequent controlled air cooling down to 370 K.

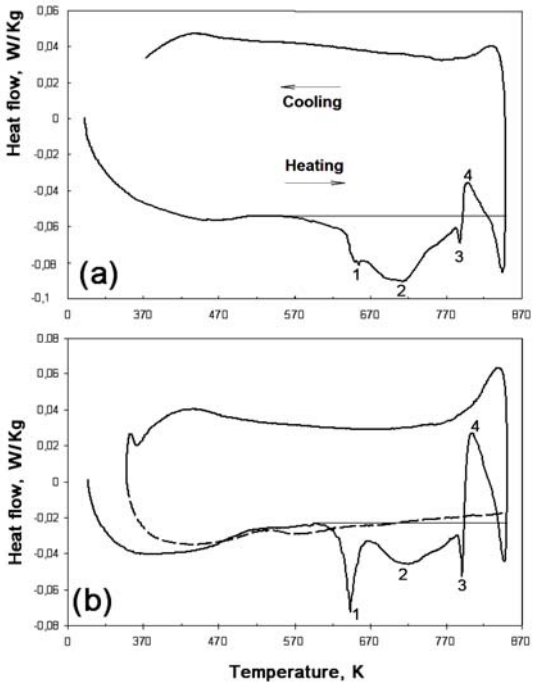

Fig. 3. DSC thermograms recorded during a heating cooling cycle up to 870 K of fragments cut from median coils of SMA springs: (a) in initial as-cast condition; (b) in trained condition, after 20 SME cycles under a 1.5 N-applied load.

It is noticeable, in Fig. 3 (b) that training amplified all the four peaks occurring on heating, suggesting an intensification of the phenomena, probably due to the contribution of stress induced martensite generated by training, which reverts to austenite concomitantly with low-temperature reversion of thermally induced martensite. Nevertheless, during cooling no solid state transition is noticeable, probably due to the same decrease of critical temperatures caused by α-phase precipitation. Moreover, since neither thermally induced nor stress-induced martensite was formed, no phase transformation occurred during the second heating. This proves that no SME can be developed unless stress induced martensite is formed or in other words unless load is applied during cooling. Considering that SME is related to low-temperature reverse martensitic transformation, it appears that thermodynamic response, sensed by DSC provides higher critical temperatures, as compared to thermomechanical response determined by SME cycling. One possible explanation for this difference could be the higher temperature variation rate used at DSC, 10×1.66

10^{-2} K/ s, as compared to $4\times1.66\ 10^{-2}$ K/ sec used during SME cycling. All critical temperatures for reverse martensitic transformation are summarized in Table 2.

Table 2. Critical temperatures for reverse martensitic transformation determined by three experimental techniques.

Experimental technique	D-T	DSC	DIL
Temperature variation rate, $1.66\ 10^{-2}$ K/ sec	4	10	5
Source	Fig. 2; 1.5 N-load	Fig. 3(b)	Fig. 4
A'_s, K	580	610	658
A'_f, K	609	675	689

In order to evaluate thermomechanical behaviour of as-cast Cu-12.89 Al-4.26 Ni (mass. %) SMA, lamellas were cut from spring assembly (Fig. 1) after casting and were analyzed by dilatometry during heating up to 870 K. The results are shown in Fig. 4.

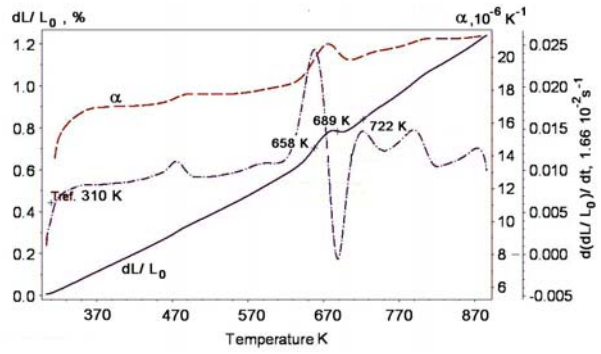

Fig. 4 Variations with temperature of relative thermal expansion (dL/ L_0 with solid line), relative thermal expansion in time $d(dL/ L_0)\ dt$) and thermal expansion coefficient (α), on the dilatogram recorded during heating to 870 K of a lamella cut from as-cast SMA springs assembly.

Considering that analyzed fragment belongs to an untrained spring, firstly low-temperature reverse transformation of thermally induced martensite is expected to occur on heating, corresponding to peak *1* in Fig. 3(a). This solid state transition is also revealed by marked fluctuations of relative thermal expansion derivative, (dL/ dt) and thermal expansion coefficient (α), between 658 and 698 K. These temperatures, listed in Table 2, would correspond to A_s and A_f, respectively. The second transformation, located at 722 K, is revealed by a smaller fluctuation of $d(dL/ L_0)\ dt$ and would correspond to high-temperature reverse martensitic transformation illustrated by peak *2* in Fig. 3. Finally, the SEM micrograph of a fragment cut from a SMA spring in as-cast condition is shown in Fig. 5.

It illustrates a typical diamond-like martensitic structure with large primary and small secondary plates. This structure characterizes the starting condition of the experiments illustrated in Fig. 3 (a) and Fig. 4 and confirms the formation of thermally induced martensite as an effect of the final step of manufacturing technology of as-cast SMA springs.

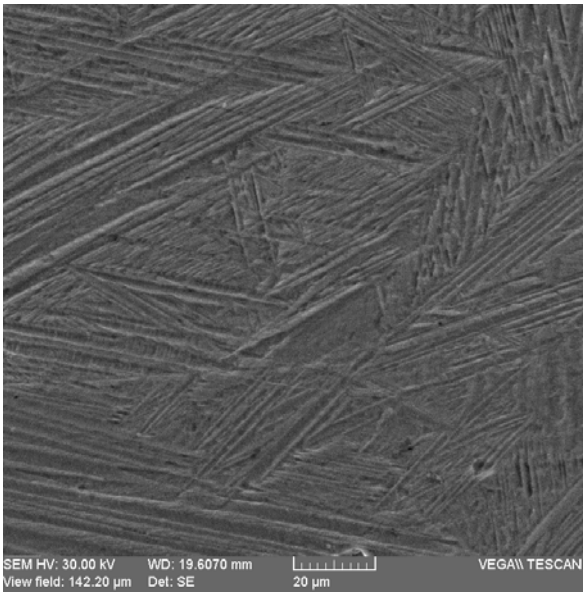

Fig. 5 SEM micrograph on a fragment cut from as-cast SMA spring.

4. Conclusions

An original manufacturing technology was introduced for obtaining Cu-12.89 Al-4.26 Ni (mass. %) SMA springs in as-cast condition, by lost wax centrifugal casting. As-cast springs, with thermally induced martensitic structure ascertained by SEM, were fully trained after 20 SME cycles, being able to develop extrinsic TWSME with 2.7 J/ kg output per mass unit. With applied-load increasing, increases of displacement variation rate with temperature, of SME-stroke as well as of critical transformation temperatures of martensite transformation were noticed on displacement-temperature curves recorded during heating-cooling up to 705 K. As compared to trained SMA springs, increases of critical transformation temperatures of thermally induced-martensite reversion to austenite, A'_s and A'_f, were emphasized both by DSC and dilatometry tests, performed on fragments cut from as-cast springs, as summarized in Table 2. When heating was applied up to 870 K, diffusion controlled transitions occurred, such as eutectoid reaction and α-phase precipitation, which rendered martensitic transformation irreversible on subsequent cooling, in the fragments cut from as-cast springs.

Acknowledgements

This work was financially supported by Romanian National University Research Council under the form of the PCE-IDEI grant 616, project 83/01.10.2007.

References

[1] T. Waram, in Engineering Aspects of Shape Memory Alloys, T. W. Duerig, K. N. Melton, D. Stöckel, C. M. Wayman, eds., Butterworth-Heinemann, 234, 1990.

[2] J. Van Humbeeck, R. Stalmans, in Shape Memory Materials, K. Otsuka, C. M. Wayman, eds., Cambridge University Press, 149, 1998.

[3] L. P. Chen, N. C. Si, J. Alloy Compd. **448**, 219 (2008).

[4] V. Dia, L. G. Bujoreanu, S. Stanciu, C. Munteanu, Mater. Sci Eng A **481-482**, 697 (2008).

[5] W. Predki, A. Knopik B. Bauer, Mater. Sci Eng A **481-482**, 598 (2008).

[6] S. Montminy, E. Dupuios, H. Champliaud, Acta Astronaut **62**, 438 (2008).

[7] J. Van Humbeeck, in Technologie des Alliagesà Mémoire de Forme, E. Patoor, M. Berveiller, Coord., Hermès, 63, 1994.

[8] E. Patoor, M. Berveiller, in Technologie des Alliages à Mémoire de Forme, E. Patoor, M. Berveiller, coord., Hermès, 195, 1994.

[9] J. Van Humbeeck, R. Stalmans, M. Chandrasekaran, L. Delaey, in Engineering Aspects of Shape Memory Alloys, T. W. Duerig, K. N. Melton, D. Stöckel, C. M. Wayman, eds., Butterworth-Heinemann, 96, 1990.

[10] G. Guenin, in Technologie des Alliages à Mémoire de Forme, E. Patoor, M. Berveiller, Coord., Hermès, 115, 1994.

[11] S. Stanciu, L. Bujoreanu, Romanian patent no. 111855C, 1998.

[12] V. Dia, L.-G. Bujoreanu, G. Hriţuleac, V. David, Bull. Inst. Polit. Iaşi, **t. LI**(LV), f. 4, s. Şt. Ing. Mater., 89 (2005).

[13] R. Stalmans, J. Van Humbeeck, L. Delaey, Acta metall. mater. **40**, 501 (1992).

[14] L. Delaey, H. Warlimont, in Shape Memory Effects in Alloys, J. Perkins, ed., Plenum Press, 89, 1975.

[15] S. Stanciu, L.-G. Bujoreanu, B. Özkal, M. L. Öveçoğlu, A. V. Sandu, J. Optoelectron. Adv. M. **10**(6), 1365 (2008).

[16] M. H. Wu, in Engineering Aspects of Shape Memory Alloys, T. W. Duerig, K. N. Melton, D. Stöckel, C. M. Wayman, eds., Butterworth-Heinemann, 69, 1990.

*Corresponding author: lgbujor@tuiasi.ro